Quantum dynamics of the intensity-dependent Tavis-Cummings model

1999 J. Phys. A: Math. Gen. 32 8739

(http://iopscience.iop.org/0305-4470/32/49/314)

J. Phys. A: Math. Gen. **32** (1999) 8739–8754. Printed in the UK PII: S0305-4470(99)02256-8

Quantum dynamics of the intensity-dependent Tavis–Cummings model

Andrei Rybin†‡, Georgii Miroshnichenko‡, Ilya Vadeiko‡ and Jussi Timonen†

† University of Jyväskylä, Department of Physics, PO BOX 35, FIN–40351 Jyväskylä, Finland
‡ Fine Mechanics and Optics Institute of St Petersburg, Sablinskaya 14, St Petersburg, 196211, Russia

E-mail: andrei.rybin@phys.jyu.fi

Received 3 March 1999, in final form 7 June 1999

Abstract. An exactly solvable generalization of the intensity-dependent Jaynes–Cummings model to the case of N_0 atoms is introduced together with its solution. The quantum dynamics of the model including the squeezing properties of the $su(1,1)$ Perelomov and Glauber coherent states is investigated. The cases of one and two atoms present in the cavity are analysed in detail. These two cases are compared in the situation when the atomic subsystem is initially prepared in the ground state, the Dicke state and the state of thermal equilibrium.

1. Introduction

In this paper we study effects of nonlinear atom–field interactions within a model whose coupling constant depends on the intensity of the field. This model, which we solve exactly, is a generalization of the intensity-dependent Jaynes–Cummings model (IDJC) to the case of N_0 atoms in the cavity, and can thus be called the *intensity-dependent Tavis–Cummings model* (IDTC). The IDJC model is a quantum model describing the interaction of a monochromatic electro-magnetic field with one two-level atom in a cavity. The Hamiltonian of this model can be expressed in the form

$$H_{ID} = \omega N + \tfrac{1}{2}\omega_0\sigma^z + \mathrm{i}g(\sqrt{N}a^\dagger\sigma^- - a\sqrt{N}\sigma^+). \tag{1}$$

Here $a^\dagger$, a are the usual operators of the Heisenberg–Weyl algebra: $[a, a^\dagger] = 1$, $a^\dagger a = N$; σ^z, $\sigma^\pm$ are Pauli matrices and ω is the frequency of the monochromatic field, while ω_0 is the resonance frequency of the two-level atom. The model equation (1) was first introduced in [1], and later analysed in [2]. A q-boson generalization of this model was introduced in [3].

As is evident from the Hamiltonian equation (1), a characteristic feature of the IDJC model is that coupling between the monochromatic field and the atom is proportional to $\sqrt{N}$. This is why the model can be called *intensity-dependent*. Admittedly this kind of coupling between the field and the atom is rather peculiar and may require further justification. In this respect it is worth mentioning that such a justification is required for any quantum-optical model based on the two-level atom approximation. The Hamiltonian describing the interaction of the two-level system with the quantized field mode should be understood as 'effective'. This means that only two atomic levels are effectively singled out from the energy spectrum. This operator includes two field operators related to the ground and excited states in question as well as an

0305-4470/99/498739+16$30.00

operator multiplier related to the dipole transition. These operators are expressed in terms of the Bose operators of the quantized field mode in a very complicated way. They should account for various Stark shifts of the quantum levels as well as for the dependence of the dipole moment of the quantum transition on the state of the exciting field. It is possible in principle to explain how to construct these effective operators for any atomic Hamiltonian and for any pair of the quantum levels using Kato's transformation operator (cf [4]) and the secular operator of degenerate perturbation theory. It is also worth mentioning that generalized Jaynes–Cummings models in general have recently become the subject of intense attention [3, 5, 6]. These considerations support the theoretical interest in the model equation (1) since this kind of interaction means effectively that the coupling constant is proportional to the amplitude of the cavity field which is a very simple case of a nonlinear interaction. Another reason for this kind of coupling is that the time evolution of all physical quantities of the IDJC model is *strictly* periodic and can be expressed in closed form rather than as an infinite series, which is usually the case for Jaynes–Cummings-type models. Thus the model equation (1) may be considered as a useful theoretical laboratory in which time evolution of a variety of initial states of the system can be analysed. This can also give insight into the behaviour of other quantum systems with strong nonlinear interactions. An interesting example of such an interaction, though different to the $\sqrt{N}$ term considered here, is the nonlinear Jaynes–Cummings dynamics of a trapped ion reported in [7, 8].

The IDJC model is also interesting because of its inherent connection to an $su(1,1)$ Jaynes–Cummings model, described by the Hamiltonian

$$H_K = \omega(K_0 - \kappa) + \tfrac{1}{2}\omega_0\sigma^z + g(K_+\sigma^- + K_-\sigma^+). \tag{2}$$

Here the operators $K_\pm$, K_0 satisfy the commutation relations of the $su(1,1)$ algebra:

$$[K_0, K_\pm] = \pm K_\pm \qquad [K_-, K_+] = 2K_0 \tag{3}$$

while κ is the so-called Bargmann index.

The connection between the models of equations (1) and (2) results from a bosonic realization of the $su(1,1)$ algebra for $\kappa = \frac{1}{2}$, namely

$$K_+ = \mathrm{i}\sqrt{N}a^\dagger \qquad K_- = -\mathrm{i}a\sqrt{N},\ K_0 = N + \tfrac{1}{2}. \tag{4}$$

This case reduces exactly to the IDJC model. The model equation (2) is also connected to the case in which atomic transitions are mediated by absorbtion and emission of two photons. This case has extensively been studied in the existing literature [9], and is found from equation (2) through another bosonic realization of the $su(1,1)$ algebra [10, 11].

The analytical formulae describing the quantum dynamics of the two-photon JC model are, however, much less transparent than those of the IDJC model. Other interesting bosonic realizations of the $su(1,1)$ algebra also exist.

In this paper we analyse the quantum dynamics and consider in particular the squeezing properties of the Perelomov [11] and Glauber [12] coherent states of the intensity-dependent Tavis–Cummings model given by the Hamiltonian

$$H = \omega N + \omega_0 S_3 + \mathrm{i}g(\sqrt{N}a^\dagger S_- - a\sqrt{N}S_+). \tag{5}$$

Notations are the same as in equation (1) apart from the operators S_3, $S_\pm$, which are the collective spin variables of N two-level atoms,

$$S_\pm = \sum_{i=1}^{N_0} \sigma_i^\pm \qquad S_3 = \tfrac{1}{2}\sum_{i=1}^{N_0} \sigma_i^3$$

that satisfy the usual $su(2)$ algebra:

$$[S_3, S_\pm] = \pm S_\pm \qquad [S_+, S_-] = 2S_3.$$

The structure of the spin-configuration space $\mathcal{H}_{N_0}$ of the atomic subsystem is given in appendix A.

As indicated above, the operators $K_\pm$ and K_0 given by equation (4) provide the particular bosonic realization of the $su(1,1)$ algebra related to the Bargmann index $\kappa = \frac{1}{2}$. Thus the quantum space $\mathcal{H}$ of the model equation (5) is given by $\mathcal{H} = \mathcal{H}_B \bigotimes \mathcal{H}_{N_0}$, where $\mathcal{H}_B$ is the space of the corresponding representation of the $su(1,1)$ algebra:

$$\begin{aligned} |n\rangle &= \frac{1}{n!}K_+^n|0\rangle \\ K_0|n\rangle &= (n+\tfrac{1}{2})|n\rangle \\ K_+|n\rangle &= (n+1)|n+1\rangle \\ K_-|n\rangle &= n|n-1\rangle. \end{aligned} \tag{6}$$

The time evolution of an initial state can be obtained by application to that state of an evolution operator $U(t)$ that can be constructed through a complete set of eigenfunctions $|\nu\rangle$ of the Hamiltonian equation (5), namely

$$U(t) = \sum_\nu |\nu\rangle\langle\nu| \exp(-\mathrm{i}E^\nu t). \tag{7}$$

Thus in order to construct the operator $U(t)$ we have to first solve the eigenvalue problem

$$H|\nu\rangle = E^\nu|\nu\rangle \tag{8}$$

where ν is a set of quantum numbers to be specified below. The eigenstates $|\nu\rangle$ are constructed in the form (for details, see [10])

$$|\nu\rangle = \sum_{n=n_0}^{M} A_{n+r}^{M,r,j}|n\rangle \otimes |M-n-r, r\rangle \tag{9}$$

for each block $\mathcal{H}_r$ in equation (40) (cf appendix A). Here the quantum number j is

$$0 \leqslant j \leqslant M - n_0 + 1 \tag{10}$$

and

$$n_0 = \max(M-2r, 0).$$

Thus the set of quantum numbers characterizing the basis of each space $\mathcal{H}_r$ for a given eigenvalue M of $\hat{M}_r$ is $\nu = (M, r, j)$.

The coefficients $\mathcal{A}_{n+r}^\nu$ are

$$\mathcal{A}_{n+r+1}^\nu = \mathcal{A}_{n_0+r}^\nu \prod_{k=n_0}^{n} c_{k+r}\, y_{k+r} \qquad n_0 \leqslant n \leqslant M-1 \tag{11}$$

where y_{k+r}, $n_0 \leqslant k \leqslant n$, are given by

$$y_{k+r} = 1 + \cfrac{d_{k+r-1}}{1 + \cfrac{d_{k+r-2}}{1 + \ddots \; 1 + \cfrac{d_{n_0+r+1}}{1+d_{n_0+r}}}} \tag{12}$$

$$d_{n+r-1} = -n^2(M-n+1)(2r-M+n)/p_n p_{n-1}. \tag{13}$$

Here

$$c_{n+r} = \frac{p_n}{(n+1)\sqrt{(M-n)(2r+1-M+n)}} \tag{14}$$

$$p_n = -\frac{1}{g}(\omega n + \omega_0(M-n-r) - E^\nu). \tag{15}$$

The eigenvalues E^{ν} of the problem equation (8) can be found from algebraic equations,

$$2rM^2 = p_M p_{M-1} y_{M+r-1}. \tag{16}$$

For the case $\omega = \omega_0$, $N = 2$, $r = 1$, and $M > 1$, e.g., these eigenvalues are

$$\begin{aligned} E^{M,1,k} &= \omega(M-1) + (-1)^k g\sqrt{2(M^2 + (M-1)^2)} \qquad k = 1, 2 \\ E^{M,1,3} &= \omega(M-1). \end{aligned} \tag{17}$$

In section 2 we apply these results to investigate the quantum dynamics for a variety of initial states of the quantum system. The properties of the Glauber and Perelomov coherent states [11] will be investigated and discussed.

2. Squeezing in the case of two atoms

We shall exemplify the application of the results given in the previous section in the simplest nontrivial case, which is that of two atoms, $N_0 = 2$, $r = 0, 1$.

For simplicity we shall only consider the case of exact resonance between the field and the two-level atom, which means $\omega_0 = \omega$, i.e. $\epsilon = 0$.

In this case the evaluation of the eigenfunctions $|\nu\rangle$ in the form of equation (14) is rather straightforward.

If $r = 0$, then $|M, 0, j\rangle = |M\rangle \otimes |0, 0\rangle$, and $j = 1$.

If $r = 1$ and $M = 0$, then $|0, 1, j\rangle = |0\rangle \otimes |-1, 1\rangle$, and $j = 1$.

If $r = 1$ and $M = 1$, then $|1, 1, j\rangle = A_2^{1,1,j}|1\rangle \otimes |-1, 1\rangle + A_1^{1,1,j}|0\rangle \otimes |0, 1\rangle$, and $j = 1, 2$.

Here

$$\begin{aligned} A_1^{1,1,j} &= (-1)^j \frac{\sqrt{2}}{2} \qquad A_2^{1,1,j} = -\frac{\sqrt{2}}{2} \\ E^{1,1,j} &= (-1)^{j+1} g\sqrt{2}. \end{aligned} \tag{18}$$

In the case $r = 1$, $M > 1$, $k = 1, 2$; $j = k, 3$; the eigenfunction is

$$\begin{aligned} |M > 1, 1, j\rangle &= A_{M+1}^{M,1,j}|M\rangle \otimes |-1, 1\rangle \\ &+ A_M^{M,1,j}|M-1\rangle \otimes |0, 1\rangle + A_{M-1}^{M,1,j}|M-2\rangle \otimes |1, 1\rangle. \end{aligned} \tag{19}$$

Notice that $\langle M > 1, 1, j | M > 1, 1, j\rangle = 1$. Here

$$\begin{aligned} A_{M-1}^{M,1,k} &= \frac{M-1}{\sqrt{2(M^2 + (M-1)^2)}} \qquad A_M^{M,1,k} = (-1)^k \frac{\sqrt{2}}{2} \\ A_{M+1}^{M,1,k} &= \frac{M}{\sqrt{2(M^2 + (M-1)^2)}} \end{aligned} \tag{20}$$

$$A_{M-1}^{M,1,3} = \sqrt{2} A_{M+1}^{M,1,k} \qquad A_M^{M,1,3} = 0 \qquad A_{M+1}^{M,1,3} = -\sqrt{2} A_{M-1}^{M,1,k}. \tag{21}$$

We shall first assume that the active atoms and the monochromatic field are initially prepared in a quantum state $|\Phi_0\rangle$,

$$|\Phi_0\rangle = |\xi\rangle \otimes \left| -\frac{N_0}{2}, \frac{N_0}{2} \right\rangle \tag{22}$$

where $|\xi\rangle$ is the Perelomov $su(1, 1)$ coherent state for $\kappa = \frac{1}{2}$, i.e.

$$|\xi\rangle = \sqrt{1 - |\xi|^2} \sum_{n=0}^{\infty} \xi^n |n\rangle \tag{23}$$

with $\xi = |\xi| e^{i\theta}$, $|\xi| \leqslant 1$, while $|-\frac{N_0}{2}, \frac{N_0}{2}\rangle$ is the ground state for the atomic subsystem.

In order to investigate the squeezing properties of these states, it is convenient to introduce the field operator

$$X(t,\varphi) = \tfrac{1}{2}(a\mathrm{e}^{\mathrm{i}(\omega t-\varphi)} + a^{\dagger}\mathrm{e}^{-\mathrm{i}(\omega t-\varphi)}). \tag{24}$$

This definition of the field operator suits well the actual method of measurement (square-law detection) of the quantized field inside the cavity [13, 14]. Notice that the time dependence introduced here has its origin in the probe field mode. This can be explained as follows. The measuring device is a balanced heterodyne detector with a local oscillator tuned to the resonance frequency ω. This method of measurement allows one to obtain the slowly varying envelopes of the dispersions rather than their rapidly (with frequency ω) oscillating parts.

Assuming that the heterodyne mode is prepared in the coherent state with a large amplitude, this mode can be considered as a classical field

$$\tfrac{1}{2}(\gamma\mathrm{e}^{-\mathrm{i}(\omega t-\varphi)} + \gamma^{*}\mathrm{e}^{\mathrm{i}(\omega t-\varphi)}). \tag{25}$$

According to the standard experimental setup, this classical oscillator mode is mixed with the cavity field which results in two side-band modes. Since the balanced heterodyne detector measures the difference of the correlation functions of these side-band modes, the output signal contains only the interference terms of the cavity and the heterodyne field components. This explains how the probe field can be excluded from the consideration provided that its time dependence is included into the cavity field. This provides us with a motivation to represent the cavity field in the form given by equation (24). Specifying the value of the angle φ, we can denote

$$\begin{aligned} X_1 &= X(t,0) \\ X_2 &= X\left(t,\frac{\pi}{2}\right). \end{aligned} \tag{26}$$

We show below (see figure 1) that this choice does not restrict the generality of our results.

As can be readily seen, the dispersions of the operators equation (26), i.e. $(\Delta X_l)^2 \equiv \langle X_l^2\rangle - \langle X_l\rangle^2$, calculated with respect to a coherent state $|\alpha\rangle$, $a|\alpha\rangle = \alpha|\alpha\rangle$, of the Heisenberg–Weyl algebra, are $(\Delta X_l)^2 = \frac{1}{4}$, $l = 1, 2$. Thus a quantum state exhibits squeezing [15] when the corresponding dispersions of the field operators fulfil the condition $(\Delta X_l)^2 \leqslant \frac{1}{4}$, either for $l = 1$ or for $l = 2$. For later convenience we introduce the quantities $S(t,\varphi) \equiv 4(\Delta X(t,\varphi))^2 - 1$ and $S_l(t) \equiv 4(\Delta X_l)^2 - 1$, such that the squeezing condition reads

$$S_l(t) \leqslant 0 \qquad \text{for} \quad l = 1 \quad \text{or} \quad l = 2. \tag{27}$$

It is also worth mentioning that, once the rapid oscillations with frequency ω are scaled out, the squeezing no longer depends on the coupling constant g that only influences the timescale of the quantum dynamics.

In the case of two atoms ($N_0 = 2$), the function $S(t,\varphi)$ takes the form

$$S(t,\varphi) = 2(C_2 - C_1^2)\cos 2(\theta-\varphi) + 2C_0 - 2C_1^2 \tag{28}$$

where

$$\begin{aligned} C_0(t) &= \frac{|\xi|^2}{1-|\xi|^2} - 1 - \langle\Phi(t)|S_3|\Phi(t)\rangle \\ |\Phi(t)\rangle &= U(t)|\Phi_0(t)\rangle \end{aligned} \tag{29}$$

while

$$\begin{aligned} \langle\Phi(t)|S_3|\Phi(t)\rangle = {} & -(1-|\xi|^2)\{1 + \tfrac{1}{2}|\xi|^2(1+\cos(2\sqrt{2}gt)) \\ & - \sum_{M=2}^{\infty}\frac{|\xi|^{2M}}{(M^2+(M-1)^2)^2}\left\{(2M-1)\left((M-1)^2 - \frac{M^2}{2}\right)\right. \end{aligned}$$

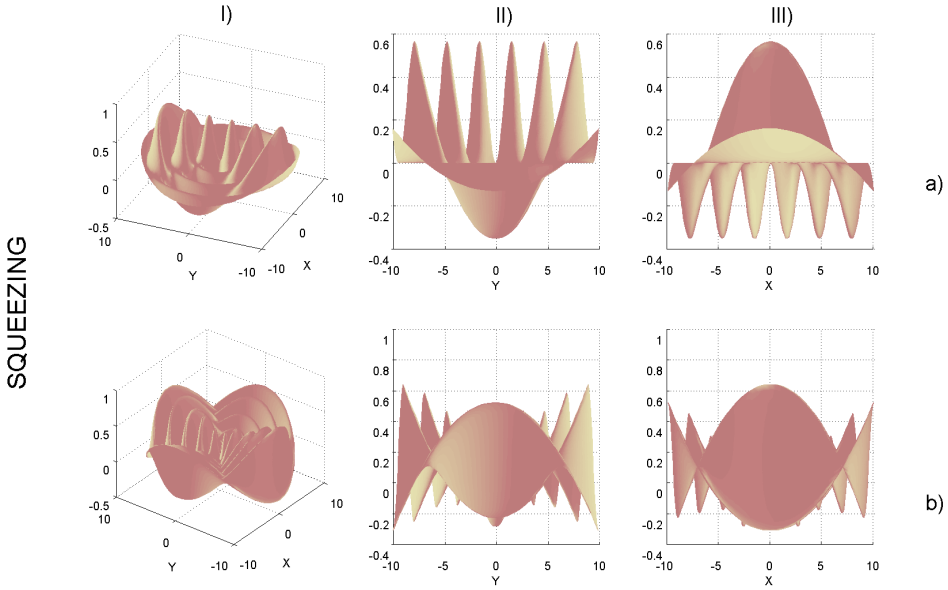

Figure 1. The plot (I) of the function $S(t,\varphi)$ in the polar coordinates ($x = t\cos\varphi$, $y = t\sin\varphi$) along with its projections on the ZY (II) and ZX (III) planes. The initial state of the field mode is the Glauber coherent state with $\alpha = 0.5e^{i\frac{\pi}{2}}$, the initial state of the atomic subsystem is as in equation (22), and $N_0 = 1(2)$ in (a) ((b)) figures.

$$-\frac{M^2}{2}(2M-1)\cos 2\sqrt{2(M^2+(M-1)^2)}gt$$
$$-4M^2(M-1)^2\cos\sqrt{2(M^2+(M-1)^2)}gt\Bigg\} \tag{30}$$

and

$$C_1(t) = ie^{-i\omega t+i\theta}\langle\Phi(t)|a^\dagger|\Phi(t)\rangle = (1-|\xi|^2)\sum_{M\geqslant 0}\sqrt{M+1}|\xi|^{2M+1} + |\xi|(1-|\xi|^2)\cos(\sqrt{2}gt)$$
$$+\operatorname{tr} Q^{(1)}P^{(1)} + \sum_{M\geqslant 2}\operatorname{tr} S^{(1)}(M)T^{(1)}(M) \tag{31}$$

$$C_2(t) = -e^{2i(\theta-\omega t)}\langle\Phi(t)|(a^\dagger)^2|\Phi(t)\rangle = (1-|\xi|^2)\sum_{M\geqslant 0}\sqrt{(M+1)(M+2)}|\xi|^{2M+2}$$
$$+\frac{\sqrt{2}}{5}|\xi|^2(1-|\xi|^2)(4\cos(\sqrt{10}gt)+1) + \operatorname{tr} Q^{(2)}P^{(2)} + \sum_{M\geqslant 2}\operatorname{tr} S^{(2)}(M)T^{(2)}(M). \tag{32}$$

The matrices $Q^{(i)}$, $P^{(i)}$, $S^{(i)}$ and $T^{(i)}$, $i = 1, 2$, are given in appendix B. Below we show in graphical form that the presence of the second atom significantly changes the dynamics of the field mode, as well as the dynamics of the atomic subsystem.

As mentioned above, we specify the value of the parameter φ in the operator equation (24) to be 0 or $\frac{\pi}{2}$. This choice is justified by figure 1, where the plots of the function $S(t,\varphi)$ in polar coordinates ($x = t\cos\varphi$, $y = t\sin\varphi$) are shown for the cases $N_0 = 1, 2$. In this figure

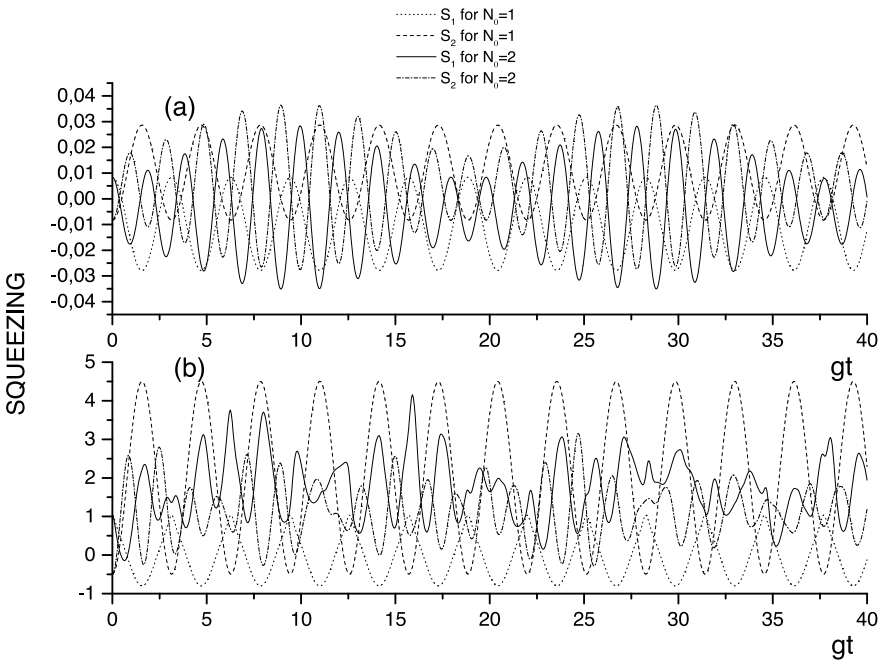

Figure 2. The behaviour as a function of time of $S_{1,2}(t)$ for $N_0 = 1, 2$ for the initial condition equation (22). Plot (*a*) corresponds to $|\xi| = 0.1$, and plot (*b*) to $|\xi| = 0.75$; $\theta = \frac{\pi}{2}$ in both graphs.

the field is assumed to be initially prepared in the Glauber coherent state

$$|\alpha\rangle = \mathrm{e}^{-\frac{|\alpha|^2}{2}} \sum_{n=0}^{\infty} \frac{\alpha^n}{\sqrt{n!}} |n\rangle \tag{33}$$

while the atomic subsystem is assumed to be in the ground state $|-r, r\rangle$ as in equation (22). Figure 1(*a*) shows that in the case $N_0 = 1$ squeezing reaches its maximum in the direction $\varphi = 0$ ($y = 0$). In the case of two atoms (figure 1(*b*)) the situation is different, since considerable squeezing can be observed both for $\varphi = 0 (y = 0)$ and for $\varphi = \frac{\pi}{2} (x = 0)$. This means that the quadratures S_1 and S_2 are well suited for studying the squeezing properties of the system. For the Perelomov coherent state $|\xi\rangle$, the plots of the function $S(t, \varphi)$ would be very similar to those given in figure 1 for the Glauber coherent state. This means that squeezing can be achieved in both cases.

The time dependences of the functions $S_1(t)$ and $S_2(t)$ for the initial state of equation (22) are shown in figure 2 for the cases of one and two atoms in the cavity. The dynamics of the quantum system in the case of two atoms, even for a relatively small number of photons in the cavity, is rather complicated. For example, the plots of the squeezing functions S_1 and S_2 in figure 2(*a*) for a low number of photons ($|\xi| = 0.1$) are quasiperiodic with a period smaller ($T_R \sim 2$) than in the case of one atom (where index R in T_R refers to similarity with the Rabi period). These functions are asymmetric with respect to the zero level and have different magnitudes of oscillation (the amplitude of S_1 is considerably bigger than that of S_2). The plots describe continuous quasiperiodic functions obtained by summing up to 30 first dominant terms in the series with respect to M given in equations (30–32). The convergence of the series is mostly governed by the factor $|\xi|^{2M}$ and is therefore rather rapid. The remainder of the series in which terms are smaller than $\mathrm{e}^{60 \ln |\xi|}$ is discarded. For comparison, the plots

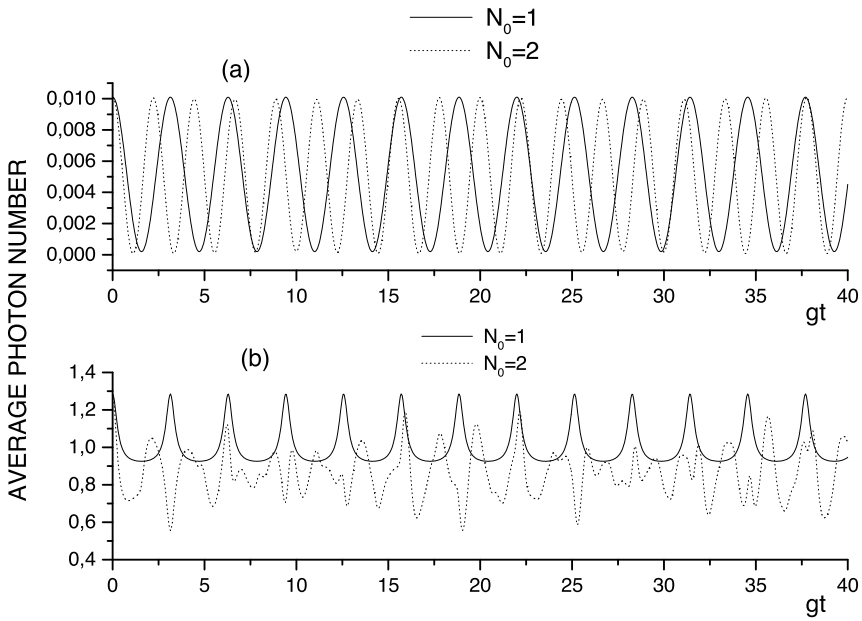

Figure 3. The average photon number for $N_0 = 1, 2$ and for the initial condition equation (22). Plot (*a*) corresponds to $|\xi| = 0.1$, and plot (*b*) to $|\xi| = 0.75$; $\theta = \frac{\pi}{2}$ in both graphs.

for the case of one atom in the cavity (the Jaynes–Cummings model) are also shown. The latter curves are periodic with the average Rabi frequency. Since the average number of photons in the cavity is low in this case (of the order of one or smaller), this period, in the chosen timescale, coincides with the classical period $T_R \sim \pi$. These amplitudes noticeably exceed the amplitude of initial squeezing of the Perelomov coherent state for both the one atom and the two atoms case. As a consequence of equation (28), the contributions proportional to $\langle\Phi(t)|a^\dagger a^\dagger|\Phi(t)\rangle$, $\langle\Phi(t)|aa|\Phi(t)\rangle$, $\langle\Phi(t)|a|\Phi(t)\rangle^2$, $\langle\Phi(t)|a^\dagger|\Phi(t)\rangle^2$ enter the function S_1 and S_2 with alternating signs, while the contributions proportional to $\langle\Phi(t)|a^\dagger a|\Phi(t)\rangle$ and $\langle\Phi(t)|a|\Phi(t)\rangle\langle\Phi(t)|a^\dagger|\Phi(t)\rangle$ enter these functions with the same sign. Evidently, the asymmetry with respect to the zero level and the different amplitudes of oscillation of the functions S_1 and S_2 are connected with the latter contributions. The plot of a part of these contributions (the average photon number in the field mode) is shown in figure 3 for $|\xi| = 0.1$ and $|\xi| = 0.75$.

The contributions connected with the average number of photons cannot explain the mentioned asymmetry, which, most probably, can be explained by the terms proportional to $\langle\Phi(t)|a|\Phi(t)\rangle\langle\Phi(t)|a^\dagger|\Phi(t)\rangle$. As is evident from figure 2(*b*) ($|\xi| = 0.75$), where the asymmetry of S_1 and S_2 is even more noticeable, the contribution of these terms increases strongly for bigger $|\xi|$. This effect is related to the fact that the initial density matrix of the field is not diagonal. To further investigate the similarities and differences in the dynamics of one and two atomic systems it is interesting to consider a slightly different state than that given by equation (22), namely

$$\rho = \tfrac{1}{2}|\xi\rangle\langle\xi| \otimes \sum_{r=0}^{1} |-r, r\rangle\langle r, -r|. \tag{34}$$

The similarity to the one-atom case arises from the fact that in this state the atoms cannot

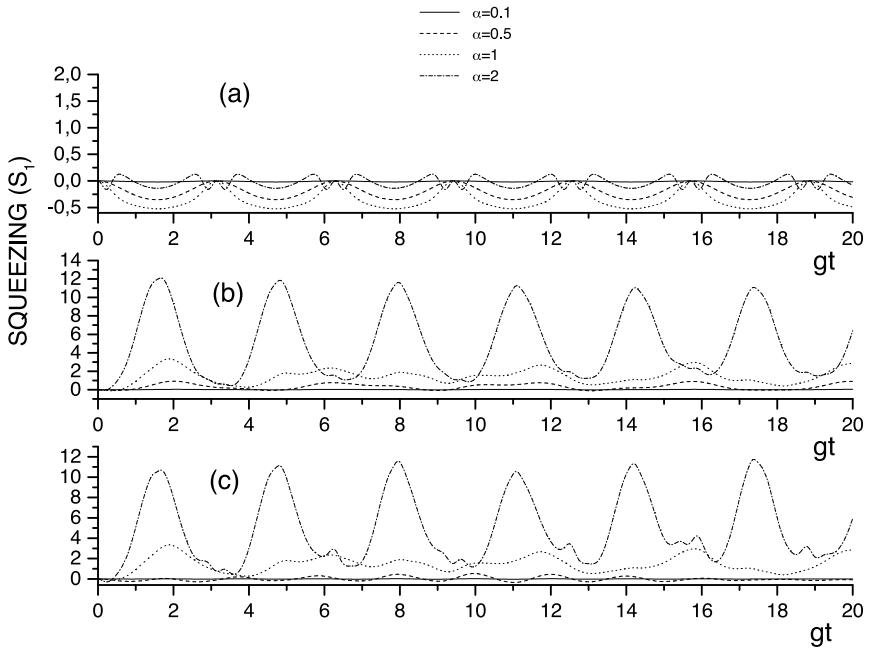

Figure 4. The behaviour as a function of time of $S_1(t)$ for $N_0 = 1, 2$. The initial condition of the atomic subsystem is: $(a)\ |-\frac{1}{2}, \frac{1}{2}\rangle$, $(b)\ \frac{1}{2}\sum_{r=0}^{1}|-r, r\rangle\langle r, -r|$ and $(c)\ |-1, 1\rangle$. The field is prepared in the coherent state $|\alpha\rangle$, $\arg(\alpha) = \frac{\pi}{2}$.

absorb on the average more than one photon. On the other hand, the structure of the quantum levels for this state remains the same as for the state equation (22). Figure 4 shows that the dynamics of the two-atom system with the initial state given by either equation (22) or equation (34) is very similar. This means that the main features of the dynamics are determined by the structure of the quantum levels rather than a possibility to store more energy. In order to thoroughly investigate how long time the field lives in the squeezed state, we introduce a function $\tau(|\xi|)$. This function can be defined as

$$\tau(|\xi|) = \lim_{T\to\infty}\frac{1}{T}\sum_{n=0}^{L+1}(t_{n+1} - t_n)\theta(-S_j(t^{(n)})). \tag{35}$$

Here $\theta(x)$ is the Heavyside step function, the set $\{t_n\}_{n=1}^{L}$ are the zeros of function $S_j(t)$ in the time interval $(0, T)$, while $t_0 = 0$ and $t_{N+1} = T$. These points may or may not be zeros of $S_j(t)$. Each of the points $t^{(n)}$ is an arbitrary point belonging to the time interval (t_n, t_{n+1}), and can be chosen, e.g., as $t^{(n)} = \frac{1}{2}(t_n + t_{n+1})$. The function $\tau(|\xi|)$ is useful since it allows us to verify the established squeezing properties in an arbitrary long timescale. The quantity $\tau(|\xi|)T_R$ shows the time within the quasiperiod within which the field can be found in the squeezed state. In figure 5 we show the 'lifetime' in the squeezed state. In this figure the initial state of the system is the same as in equation (34).

The spin configuration given in equation (34) can be prepared as follows. Let us consider a two-atom state in which one atom is excited while the other is in the ground state. Should we be able to distinguish which atom is the excited one before they enter the cavity, the spin configuration of the atoms would be described by the state

$$|\Phi_{at}\rangle = \frac{\sqrt{2}}{2}|0, 1\rangle \pm \frac{\sqrt{2}}{2}|0, 0\rangle.$$

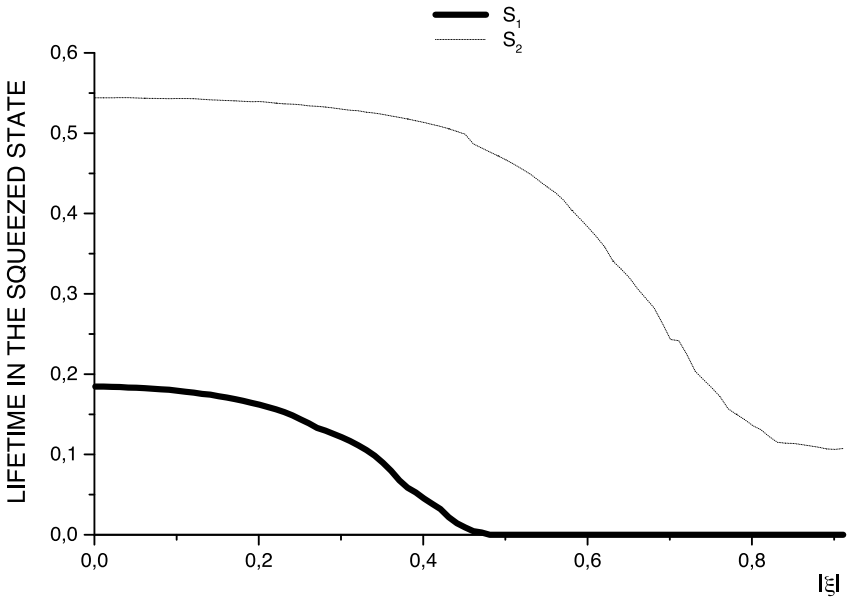

Figure 5. The lifetime in the squeezed state $\tau(|\xi|)$ for $S_{1,2}$, $N_0 = 2$, and for the initial condition equation (34); $\theta = \frac{\pi}{2}$.

The triplet state $|m, 1\rangle$ would decay with an exponential rate to the ground state $|-1, 1\rangle$ while the singlet state $|0, 0\rangle$ would remain intact since it does not interact with the field. This means that the density matrix of the pure state $|\Phi_{at}\rangle\langle\Phi_{at}|$ would evolve into that of the mixed state equation (34). This method was proposed by Dicke in [18].

Figure 5 shows the threshold for squeezing in the quadrature S_1 with respect to the parameter $|\xi|$ of the Perelomov state, while the quadrature S_2 does not show squeezing but approaches a constant nonzero value for increasing $|\xi|$. The latter effect demonstrates the independence of S_2 on the number of photons in the field mode provided that this number is big enough. It should be mentioned that this difference in the behaviour of the lifetimes of S_1 and S_2 is connected with the chosen value of the phase of the Perelomov parameter ξ ($\theta = \frac{\pi}{2}$). The introduced function τ ensures that, by adjusting the parameter θ, it is possible to guarantee the existence of squeezing, (and vice versa its absence for another quadrature) for arbitrarily late times.

It is also evident from figure 5 that the dynamics of the system is divided into three different regions. These regions are related to the amount of the energy stored in the system. The first region appears for $|\xi| \leqslant 0.2$–0.3, i.e. at small energies, the second one for $0.3 \leqslant |\xi| \leqslant 0.8$, which means an intermediate amount of energy, and the third one appears for $0.8 \leqslant |\xi|$ when the energy stored in the system is fairly large. The exact boundaries of these regions depend on the parameters of the initial state of the system such as, e.g., the phase θ of the Perelomov coherent state. In the first and the third regions all physical observables in the two-atom case have almost periodic time dependences, and their dynamics is very similar to that in the one-atom case. In the intermediate region however the dynamics in the case of two atoms significantly differs from the dynamics of the IDJC model and becomes much less periodic. This phenomenon can also be observed in the two-atom system in figures 2 and 3 which show squeezing and the average photon number in this case. The explanation of this phenomenon is the following. In the first region the field does not have energy to sufficiently excite the

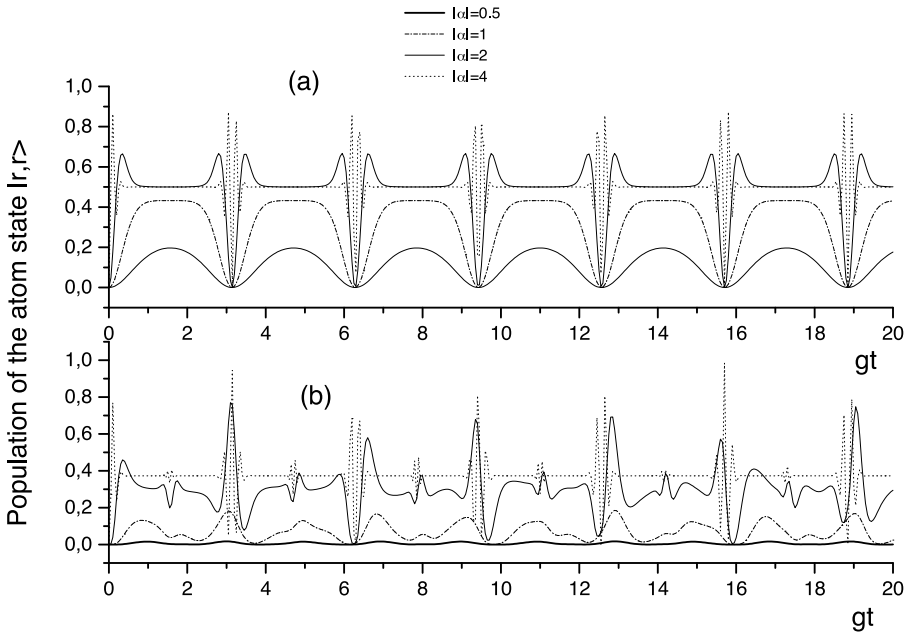

Figure 6. The population of the upper state $|r, r\rangle$ for (*a*) $N_0 = 1$, $r = \frac{1}{2}$ and (*b*) $N_0 = 2$, $r = 1$; $\arg(\alpha) = \frac{\pi}{2}$.

atomic subsystem. The periodic behaviour in the third region is explained by the fact that the atomic subsystem cannot absorb more than one or two photons in the one-and two-atom cases, respectively. To support this explanation we have also plotted in figure 6 the dynamics of the population of the excited state $|1, 1\rangle$. In figure 6 the field is initially prepared in the Glauber coherent state equation (33) with different average numbers of photons given by $|\alpha|^2$. In the case of two atoms, the population of the state $|1, 1\rangle$ has an upper boundary equal to 1.

Let us now consider the situation when the atomic subsystem is initially prepared in the state of thermal equilibrium with temperature T_{at}, while the field is in the Glauber coherent state $|\alpha\rangle$. The overall density matrix of the system is

$$\rho = \rho_f \otimes \rho_{at} \tag{36}$$

with

$$\begin{aligned} &\rho_f = |\alpha\rangle\langle\alpha| \qquad \rho_{at} = \frac{1}{Z}\sum_{r=\epsilon_{N_0}}^{N_0/2} k_r \sum_{m=-r}^{r} |m, r\rangle\langle r, m|\mathrm{e}^{-m\beta} \\ &Z = \sum_{r=\varepsilon_{N_0}}^{\frac{N_0}{2}} k_r \frac{\mathrm{e}^{-\beta(r+1)} - \mathrm{e}^{\beta r}}{\mathrm{e}^{-\beta} - 1} \end{aligned} \tag{37}$$

and

$$\beta = \frac{\omega}{kT_{at}}.$$

The matrix elements of the density matrix (36) are given by

$$\langle n| \otimes \langle r, m|\hat{\rho}|m', r'\rangle \otimes |n'\rangle = \mathrm{e}^{-|\alpha|^2} \frac{\alpha^n (\alpha^*)^{n'}}{\sqrt{n! \cdot n'!}} \cdot \delta_{m,m'}\delta_{r,r'} \frac{\mathrm{e}^{-\beta}}{Z}. \tag{38}$$

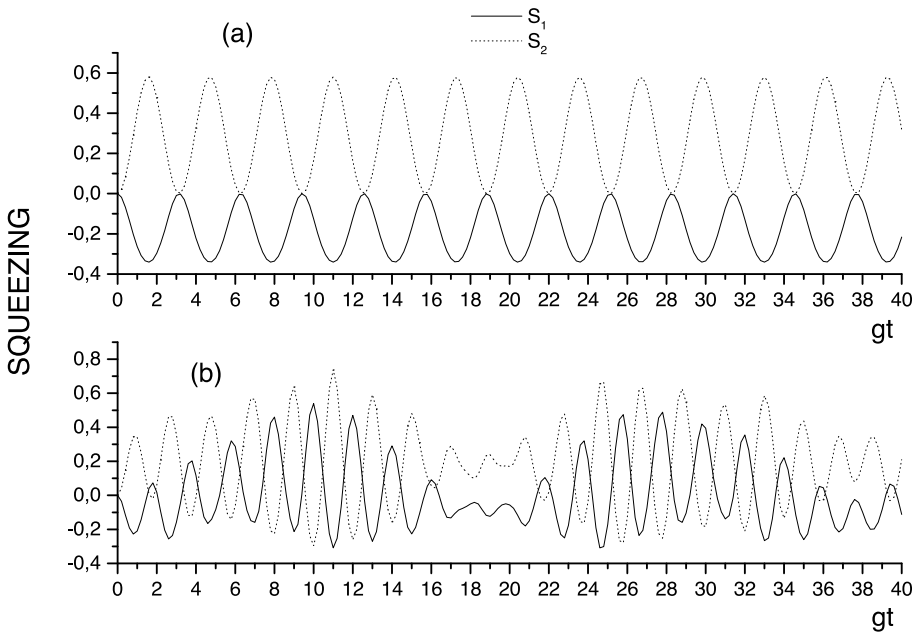

Figure 7. The behaviour as a function of time of $S_{1,2}(t)$ for (*a*) $N_0 = 1$ and (*b*) $N_0 = 2$, and for the initial condition equation (36); $\beta = 5$, $|\alpha| = 0.5$, $\arg(\alpha) = \frac{\pi}{2}$.

Because of the long and cumbersome analytical expressions involved, we do not report here on the evaluation of the quadratures for the initial condition equation (36). We find it more convenient instead, with symbolic computer languages available, to develop a software which allows us to derive all the necessary physical quantities. For this we used the MathCAD program. Squeezing found for the initial condition equation (36) is shown in figures 7 and 8. We considered two different situations. In figure 7 we show squeezing in the case when the average energy in the atomic subsystem is initially larger than in the field mode. In figure 8 we consider the opposite situation. The energy stored in the atomic subsystem at $t = 0$ is given by

$$E_{at}(t = 0) = \frac{N_0}{1 + \mathrm{e}^{\beta}} \tag{39}$$

while the field energy is given by $E_f(t = 0) = |\alpha|^2$. Notice that the energy is measured in units of ω. In figure 7 $\beta = 5$, $E_{at}(t = 0) = 0.538$ for $N_0 = 2$, and $E_{at}(t = 0) = 0.269$ for $N_0 = 1$. In figure 8 $\beta = 1$, $E_{at}(t = 0) = 0.013$ for $N_0 = 2$, and $E_{at}(t = 0) = 6.693 \times 10^{-3}$ for $N_0 = 1$. It clear that if the energy stored in the atomic subsystem is less than the energy stored in the field mode, squeezing appears in both the one- and two-atom cases. However, when the temperature of the atoms is such that their average energy is greater than the energy of the field, no squeezing can be observed even in the one-atom case. It is interesting to notice that in the one-atom case both field quadratures reach zero, with the same period. In the case of two atoms the picture is more complex, but some kind of period T_R can still be identified in S_2.

3. Conclusions

In this paper we have continued our investigation of the $su(1, 1)$ Tavis–Cummings model which we introduced in [10]. The chosen boson realization of the $su(1, 1)$ algebra led us

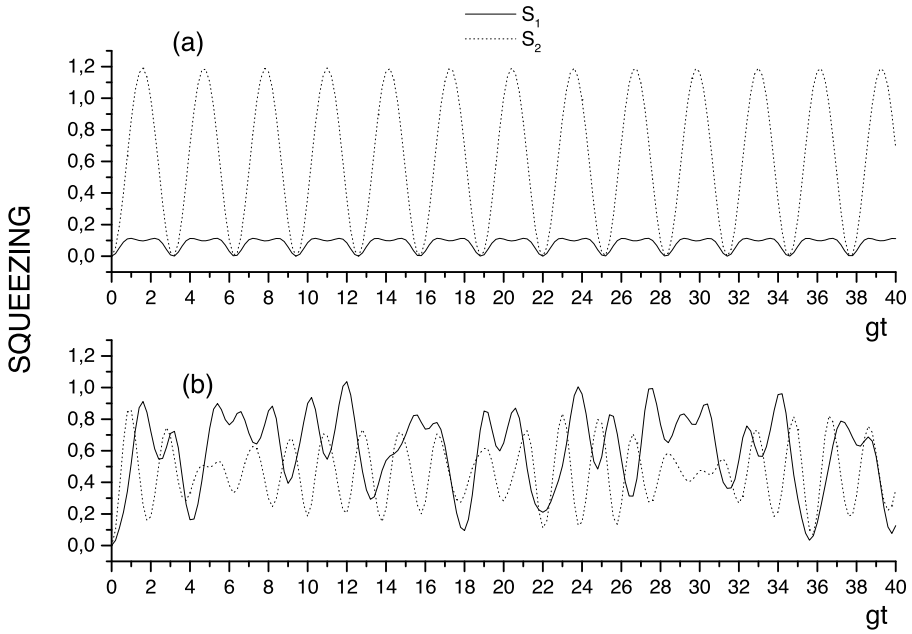

Figure 8. The behaviour as a function of time of $S_{1,2}(t)$ for (*a*) $N_0 = 1$ and (*b*) $N_0 = 2$, and for the initial condition equation (36); $\beta = 1$, $|\alpha| = 0.5$, $\arg(\alpha) = \frac{\pi}{2}$.

to an intensity-dependent Tavis–Cummings model. This model we solved exactly for the eigenfunctions and eigenvalues of the Hamiltonian of the model. This allowed us to investigate in detail the quantum dynamics of the model. The motivation for this study was to investigate, in particular, the influence of a nonlinear interaction (the intensity-dependent coupling) on the quantum dynamics and, more specifically, on the squeezing properties. We restricted our analysis to the case when the field is initially prepared in the Perelomov or Glauber coherent state which are most common in the literature on the IDJC model, while the atomic subsystem is either in thermal equilibrium or in the ground state. For these initial states we obtained the time behaviour of the average photon number and the population of the ground state, and investigated the squeezing properties of the field states. The cases of one and two atoms present in the cavity were analysed and compared. We also introduced a function which shows the lifetime of the field in the squeezed state for an infinitely long time interval. This function proved to be useful when analysing the conditions under which squeezing can be observed. The reported analysis will be very helpful in the investigation, e.g., of the two-photon micromaser in the case when there are many atoms present in the cavity at any given instant. The model of this problem is again given by the $su(1, 1)$ Tavis–Cummings model, based, however, on a different boson realization of the $su(1, 1)$ algebra. Notice also that the importance of cooperative effects for the operation of the micromaser needs further clarification. In this and our previous work [10] we have developed methods that should help us better understand these cooperative effects on the operation of the two-photon, N_0-atom micromaser. Work in this direction is now in progress.

Acknowledgments

It is our pleasure to thank V P Smirnov and M Lindberg for useful discussions. GM and IV thank the Department of Physics, University of Jyväskylä, for their warm hospitality at the final stage of the work.

Appendix A

Up to minor details the structure of the quantum space of the model coincides with that of the conventional Tavis–Cummings model [19]. Namely, the quantum space of the system of N_0 two-level atoms $\mathcal{H}_{N_0}$ is given by

$$\mathcal{H}_{N_0} = \bigoplus k_r \mathcal{H}_r \qquad r = \frac{N_0}{2} \quad \frac{N_0}{2} - 1, \ldots, \varepsilon_{N_0} \tag{40}$$

where $\varepsilon_{N_0} = \frac{1}{4}(1 - (-1)^{N_0})$. Here r is Dicke's occupation number, $\mathcal{H}_r \simeq \mathcal{C}^{2r+1}$ is a complex space of dimension $(2r+1)$ corresponding to an irreducible representation of the $su(2)$ algebra given by

$$\begin{aligned} &|m, r\rangle = \left(\frac{(r-m)!}{(r+m)!(2r)!}\right)^{\frac{1}{2}} (S_+)^{r+m} |-r, r\rangle \\ &S_\pm |m, r\rangle = \sqrt{r(r+1) - m(m \pm 1)}\,|m \pm 1, r\rangle \\ &S_3 |m, r\rangle = m|m, r\rangle \\ &S^2 |m, r\rangle = r(r+1)|m, r\rangle \end{aligned} \tag{41}$$

with $S^2 = (S_3)^2 + \frac{1}{2}(S_+S_- + S_-S_+)$.

In equation (40) the number k_r,

$$k_r = \frac{N_0!(2r+1)}{(\frac{1}{2}N_0 + r + 1)!(\frac{1}{2}N_0 - r)!}$$

reflects the multiplicity of choices which can be used to create an atomic configuration with given quantum numbers r.

Appendix B

Here we give the exact forms of matrices $Q^{(i)}$, $P^{(i)}$, $S^{(\mathrm{i})}$ and $T^{(\mathrm{i})}$, $\mathrm{i} = 1, 2$.

Matrices $S^{(1)}(M)$, $Q^{(1)}(M)$, $P^{(1)}(M)$ are given by

$$S^{(1)}(M) = \mathrm{e}^{\mathrm{i}t(E^{M+1,1,j'} - E^{M,1,j} - \omega)} \qquad j, j' = 1, 2 \tag{42}$$

$$Q^{(1)} = |\xi|^3(1 - |\xi|^2) \begin{pmatrix} \frac{-\sqrt{5}}{10} + \frac{\sqrt{2}}{5} & \frac{\sqrt{5}}{10} + \frac{\sqrt{2}}{5} & \frac{\sqrt{2}}{10} \\ \frac{\sqrt{5}}{10} + \frac{\sqrt{2}}{5} & \frac{-\sqrt{5}}{10} + \frac{\sqrt{2}}{5} & \frac{\sqrt{2}}{10} \end{pmatrix} \tag{43}$$

$$P^{(1)} = \begin{pmatrix} \mathrm{e}^{-\mathrm{i}(\sqrt{10}+\sqrt{2})gt} & \mathrm{e}^{\mathrm{i}(-\sqrt{10}+\sqrt{2})gt} \\ \mathrm{e}^{\mathrm{i}(\sqrt{10}-\sqrt{2})gt} & \mathrm{e}^{\mathrm{i}(\sqrt{10}+\sqrt{2})gt} \\ \mathrm{e}^{-\mathrm{i}\sqrt{2}gt} & \mathrm{e}^{\mathrm{i}\sqrt{2}gt} \end{pmatrix}. \tag{44}$$

Matrix $T^{(1)}(M)$ can be expressed in the form

$$T^{(1)}(M)_{j,j'} = |\xi|^{2M+1}(1 - |\xi|^2) t^{(1)}_{j,j'} \qquad j, j' = 1, 2, 3 \tag{45}$$

where

$$t^{(1)}_{k,k'} = \frac{M(M+1)}{4[(M+1)^2 + M^2][M^2 + (M-1)^2]}$$

$$\times\left\{M(M-1)^{\frac{3}{2}}+(-1)^{k+k'}\sqrt{M[M^2+(M-1)^2][(M+1)^2+M^2]}\right.$$
$$\left.+M(M+1)^{\frac{3}{2}}\right\}\quad \text{for } k,k'=1,2 \tag{46}$$

and, otherwise,

$$t^{(1)}_{k,3}=-\frac{M^2}{2[(M+1)^2+M^2][M^2+(M-1)^2]}\times\left[(M^2-1)\sqrt{M-1}-M^2\sqrt{M+1}\right]$$
$$t^{(1)}_{3,k'}=-\frac{M^2-1}{2[(M+1)^2+M^2][M^2+(M-1)^2]}\times\left[M^2\sqrt{M-1}-(M^2-1)\sqrt{M+1}\right] \tag{47}$$
$$t^{(1)}_{3,3}=\frac{M^2(M-1)}{[(M+1)^2+M^2][M^2+(M-1)^2]}\times\left[(M+1)\sqrt{M-1}+(M-1)\sqrt{M+1}\right].$$

Matrices $Q^{(2)}$, $P^{(2)}$

$$Q^{(2)}=|\xi|^4(1-|\xi|^2)\begin{pmatrix}\frac{-3\sqrt{26}+9\sqrt{6}}{52} & \frac{3\sqrt{26}+9\sqrt{6}}{52} & \frac{2\sqrt{6}}{13}\\ \frac{3\sqrt{26}+9\sqrt{6}}{52} & \frac{-3\sqrt{26}+9\sqrt{6}}{52} & \frac{2\sqrt{6}}{13}\end{pmatrix} \tag{48}$$
$$P^{(2)}=\begin{pmatrix}\mathrm{e}^{-\mathrm{i}(\sqrt{26}+\sqrt{2})gt} & \mathrm{e}^{\mathrm{i}(-\sqrt{26}+\sqrt{2})gt}\\ \mathrm{e}^{\mathrm{i}(\sqrt{26}-\sqrt{2})gt} & \mathrm{e}^{\mathrm{i}(\sqrt{26}+\sqrt{2})\mathrm{g}t}\\ \mathrm{e}^{-\mathrm{i}\sqrt{2}\mathrm{g}t} & \mathrm{e}^{\mathrm{i}\sqrt{2}gt}\end{pmatrix} \tag{49}$$

while the elements of matrix $S^{(2)}(M)$ are given by

$$S^{(2)}(M)_{k'k}=\exp\left(\mathrm{i}\left[(-1)^{k'}\sqrt{4M^2+12M+10}+(-1)^k\sqrt{4M^2-4M+2}\right]gt\right) \tag{50}$$

for $k,k'=1,2$, and

$$S^{(2)}(M)_{3,k}=\exp\left(\mathrm{i}(-1)^k\sqrt{4M^2-4M+2}gt\right)$$
$$S^{(2)}(M)_{k',3}=\exp\left(\mathrm{i}(-1)^{k'}\sqrt{4M^2+12M+10}gt\right) \tag{51}$$
$$S^{(2)}(M)_{3,3}=1.$$

The elements of matrix $T^{(2)}$ can be expressed in the form

$$T^{(2)}=(1-|\xi|^2)|\xi|^{2M+2}t^{(2)}(M) \tag{52}$$

where

$$t^{(2)}_{k,k'}=\frac{M(M+2)}{4[M^2+(M-1)^2][(M+2)^2+(M+1)^2]}$$
$$\times\left\{(M^2-1)\sqrt{M(M-1)}\right.$$
$$+(-1)^{k+k'}\sqrt{M(M+1)[M^2+(M-1)^2][(M+2)^2+(M+1)^2]}$$
$$\left.+M(M+2)\sqrt{(M+2)(M+1)}\right\}\quad \text{for}\quad k,k'=1,2 \tag{53}$$

and, otherwise,

$$
\begin{aligned}
t^{(2)}_{k,3} &= -\frac{M(M+1)}{2[M^2+(M-1)^2][(M+2)^2+(M+1)^2]} \\
&\quad\times\left[(M-1)(M+2)\sqrt{M(M-1)}-M(M+1)\sqrt{(M+2)(M+1)}\right] \\
t^{(2)}_{3,k'} &= -\frac{(M-1)(M+2)}{2[M^2+(M-1)^2][(M+2)^2+(M+1)^2]} \\
&\quad\times\left[M(M+1)\sqrt{M(M-1)}-(M+2)(M-1)\sqrt{(M+2)(M+1)}\right] \\
t^{(2)}_{3,3} &= \frac{M^2-1}{[M^2+(M-1)^2][(M+2)^2+(M+1)^2]} \\
&\quad\times\left[M(M+2)\sqrt{M(M-1)}+(M^2-1)\sqrt{(M+2)(M+1)}\right].
\end{aligned}
\tag{54}
$$

References

[1] Buck B and Sukumar C V 1981 *Phys. Lett.* A **81** 132
[2] Bužek V 1989 *Phys. Rev.* A **39** 3196
[3] Chaichian M, Ellinas D and Kulish P 1990 *Phys. Rev. Lett.* **65** 980
[4] Kato T 1966 *Perturbation Theory for Linear Operators* (Berlin: Springer)
[5] Tang Zh 1995 *Phys. Rev.* A **52** 3448
[6] Bonatsos D, Daskaloyannis C and Lalazissis G A 1993 *Phys. Rev.* A **47** 3448
[7] Vogel W and de Matos Filho R L 1995 *Phys. Rev.* A **52** 4214
[8] Blockey C A, Walls D F and Risken H 1992 *Europhys. Lett.* **17** 509
[9] Gerry C C 1988 *Phys. Rev.* A **37** 2683
[10] Rybin A, Kastelewicz G, Timonen J and Bogoliubov N 1998 *J. Phys. A: Math. Gen.* **31** 4705
[11] Perelomov A M 1972 *Commun. Math. Phys.* **26** 222
[12] Glauber R G 1963 *Phys. Rev.* **131** 2766
Glauber R G 1963 *Phys. Rev. Lett.* **10** 84
[13] Yuen H P and Chan V W S 1983 *Opt. Lett.* **8** 177
[14] Slusher R E, Hollberg L W, Yurke B, Mertz J C and Valley J F 1985 *Phys. Rev. Lett.* **55** 2409
Ling-An Wu, Kimble H J, Hall J L and Wu H 1986 *Phys. Rev. Lett.* **57** 2520
[15] Wódkiewicz K and Eberly J H 1985 *J. Opt. Soc. Am.* B **2** 458
[16] Yuen H P 1976 *Phys. Rev.* A **13** 2226
Yurke B 1984 *Phys. Rev.* A **29** 408
Collet M J and Walls D F 1985 *Phys. Rev.* A **32** 2887
[17] Bužek V 1989 *Phys. Lett.* **139** 231
[18] Dicke R H 1954 *Phys. Rev.* **93** 99
[19] Tavis M and Cummings F W 1968 *Phys. Rev.* **170** 379